Micelle Formation and Inversion Kinetics of a Schizophrenic Diblock Copolymer

Di Wang,[†] Jun Yin,[†] Zhiyuan Zhu,[†] Zhishen Ge,[†] Hewen Liu,[†] Steven P. Armes,[‡] and Shiyong Liu*,[†]

Department of Polymer Science and Engineering, the Hefei National Laboratory for Physical Sciences at Microscale, University of Science and Technology of China, Hefei, 230026, Anhui Province, China, and Department of Chemistry, University of Sheffield, Brook Hill, Sheffield, South Yorkshire, S3 7HF, U.K.

ABSTRACT: It is known that the zwitterionic diblock copolymer, poly(4-vinylbenzoic acid)-*b*-poly(*N*-(morpholino)ethyl methacrylate) (VBA-*b*-MEMA), exhibits interesting "schizophrenic" micellization behavior (see: Liu, S.; Armes, S. P. *Langmuir* **2003,** *19,* 4432–4438). The kinetics of the pH-induced formation and dissociation of VBA−core micelles, the salt-induced formation and dilution-induced dissociation of MEMA−core micelles at pH 10, and the pH-induced micellar inversion between VBA− and MEMA−core micelles in the presence of 0.8 M Na$_2$SO$_4$ were studied in detail using stopped-flow apparatus equipped with a light scattering detector. A pH jump from 12 to 2 in the absence of salt leads to the formation of VBA−core micelles; upon a pH jump from 2 to 12, the breakup of VBA−core micelles into unimers occurs within the dead time of the stopped-flow apparatus ($\sim$ 2–3 ms). At pH 10, addition of Na$_2$SO$_4$ (> 0.6 M) induces the formation of MEMA−core micelles. Compared to the pH-induced formation and dissociation of VBA−core micelles, the salt-induced formation of MEMA−core micelles is faster, while the dilution-induced dissociation of MEMA−core micelles into unimers is considerably slower. This partially reflects the block length asymmetry of this VBA-*b*-MEMA copolymer and also the fact that the MEMA−core micelles are denser and larger than the VBA−core micelles. The structural inversion from VBA−core micelles to MEMA−core micelles upon a pH jump from 2 to 12 in the presence of 0.8 M Na$_2$SO$_4$ proceeds first with the fusion of VBA−core micelles into lose aggregates due to the insolubility of MEMA shell immediately after pH jump, then the dissociation of VBA−core micelles into unimers and partial disintegration of initially formed loose aggregates, which is followed and/or accompanied by the reaggregation of unimer chains into MEMA core-micelles. The structural inversion from MEMA−core micelles to VBA−core micelles on jumping from pH 12 to 2 in the presence of 0.8 M Na$_2$SO$_4$ exhibits different kinetics. The scattering intensities decrease monotonically with time and then stabilize out. All the relaxation curves at different copolymer concentrations can be well-fitted using a single-exponential function and the characteristic relaxation time for the structural inversion of the micelles (τ_i) is $\sim$0.3 s, which slightly decreases with increasing copolymer concentrations. We tentatively propose that the structural inversion from MEMA−core to VBA−core micelles proceeds first with the splitting of large MEMA−core micelles into small VBA−core micelles, followed and/or accompanied by the redistribution of unimer chains between appearing small VBA−core micelles.

Introduction

Like small molecule surfactants, amphiphilic block copolymers can form both conventional micelles and so-called "inverted" micelles in aqueous and organic solvents, respectively.[1−6] In the past few years, increasing attention has been paid to the so-called "double hydrophilic" block copolymers (DHBCs).[7−21] Moreover, given judicious adjustment of the solution pH, temperature, or ionic strength, certain DHBCs can self-assemble in aqueous solution to form two types of micelles.[8−14,17,19−23] We have described such DHBCs as having "schizophrenic" character.[19] However, nearly all reports of stimuli-responsive micellization and micellar inversion of DHBCs focus on the characterization of the *equilibrium* micelle structures.[7−23]

Theoretical and experimental studies of the dynamics of micellization are quite mature and well-developed for conventional surfactants.[24−30] It is generally accepted that a small perturbation leads to relaxation from the initial equilibrium state to the final state via two successive processes. A fast process (τ_1) is associated with the redistribution of the aggregation number of each micelle without changing the total number of micelles. This is followed by a slower process (τ_2), in which the final equilibrium structure is approached by simultaneous micelle formation and breakup whereby the micelle number density changes. This is the well-known A−W theory proposed by Aniansson and Wall (A−W).[24−26] An important assumption in this theory is that all changes are due to an elementary process of insertion/expulsion of individual chains ("unimers") into/out of the micelle. For the slower process (τ_2), i.e., micelle formation and breakup, it has been postulated that micelle fusion−fission may also be involved, especially at higher concentrations or in the presence of salt.[27,28] Strong evidence for a micelle fusion−fission mechanism comes from the decreasing τ_2 with increasing concentration.

For block copolymers, the characteristic relaxation time for a copolymer chain to escape from the micelles has been theoretically discussed by Halperin and Alexander on the basis of scaling analysis within the context of the A−W theory.[31] Their main conclusion is that insertion/expulsion of individual chains (unimer exchange) is the only mechanism for block copolymer micelle evolution. It should be noted that this

* To whom correspondence should be addressed. E-mail: sliu@ustc.edu.cn
† Department of Polymer Science and Engineering, the Hefei National Laboratory for Physical Sciences at Microscale, University of Science and Technology of China.
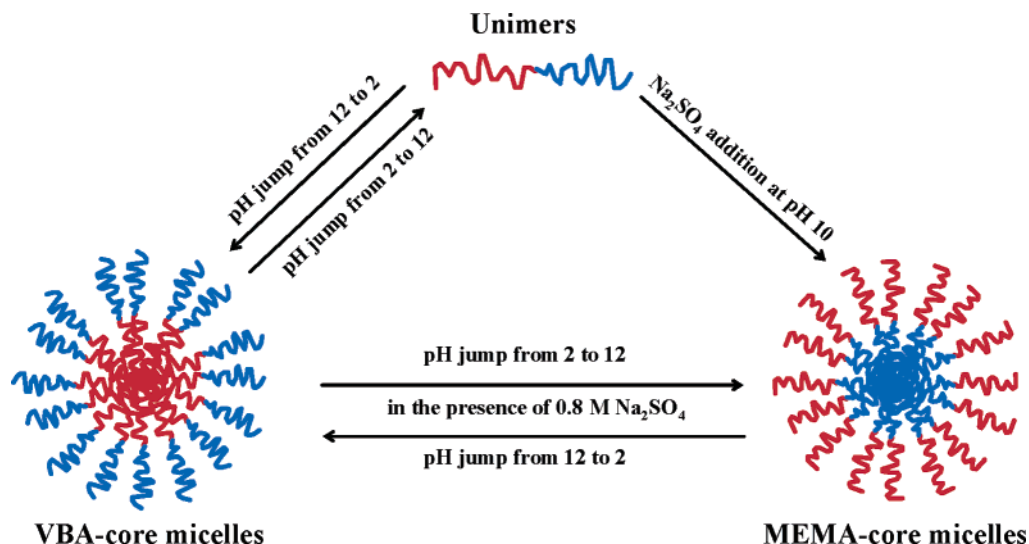‡ Department of Chemistry, University of Sheffield.

CDV

Figure 1. Schematic illustration of the "schizophrenic" micellization behavior of VBA-*b*-MEMA diblock copolymer.

assumption is only valid for small deviations from the initial equilibrium state. Extensive temperature jump (typically $\Delta T = 1-2$ °C) experiments conducted on $E_nP_mE_n$ triblock copolymers (where E_n = poly(ethylene oxide) and P_m = poly(propylene oxide)) using light scattering detection have partially verified the proposed micellization dynamics.[32-38] However, there exist evidences that micelle fission–fusion may also play an important role,[35-38] which is contrary to Halperin and Alexander's predictions.[31]

For the unimer-to-micelle transition of block copolymers, Mattice et al.[39] performed computer simulations that suggest the presence of two processes with different time scales: the volume fraction of free chains reaches its equilibrium value very quickly in the fast step, followed by a slower step toward the equilibrium state. Dormidontova and co-workers[40-42] further proposed a micelle fusion/fission–unimer expulsion/entry joint mechanism for the formation of block copolymer micelles whereby rapid micelle fusion/fission dominates over unimer entry/expulsion initially, while the latter (slow) process dominates on longer time scales.

Experimentally, there are only a few reports of the micellization kinetics (unimer-to-micelle transition) of block copolymers.[43-47] A generally accepted mechanism for the micellization process has not been established yet. Recently, we reported the kinetics of pH-induced micellization of a stimulus-responsive ABC triblock copolymer, namely poly(glycerol monomethacrylate)-*block*-poly(2-(dimethylamino)ethyl methacrylate)-*block*-poly(2-(diethylamino)ethyl methacrylate) (GMA-*b*-DMA-*b*-DEA).[47] This triblock copolymer molecularly dissolves in aqueous solution at pH < 6. At pH > 7, it spontaneously forms three layer "onionlike" micelles consisting of DEA cores, solvated DMA inner shells, and GMA outer coronas. The kinetics of micellization of this copolymer was investigated by stopped-flow light scattering. On jumping from pH 4 to 12, micellization occurred via two successive processes. The first fast process (τ_1) is associated with the formation of quasi-equilibrium micelles and the second slow process (τ_2) is associated with micelle formation and breakup, leading to the formation of the final equilibrium micelles. In this case, τ_2 is almost independent of polymer concentration, indicating that the slow process of micelle formation/breakup proceeds mainly through the insertion/expulsion of individual chains.[47]

We have previously reported the "schizophrenic" micellization behavior of a zwitterionic diblock copolymer, poly(4-vinylbenzoic acid)-*b*-poly(*N*-(morpholino)ethyl methacrylate) (VBA-*b*-MEMA).[21] In the absence of salt, this copolymer molecularly dissolves in water at high pH and forms VBA–core micelles at low pH. In the presence of 0.8 M Na_2SO_4, well-defined VBA–core and MEMA–core micelles are formed in acidic and alkaline media, respectively. Figure 1 shows a schematic illustration of this complex micellization behavior. Herein we investigate the kinetics of pH-induced formation and dissociation of VBA–core micelles, the salt-induced formation and dilution-induced dissociation of MEMA–core micelles at pH 10, and the pH-induced structural inversion between VBA–core and MEMA–core micelles in the presence of 0.8 M Na_2SO_4 using stopped-flow light scattering technique.

Experimental Section

Materials. 4-Vinylbenzoic acid was synthesized from 4-carboxybenzyltriphenyl phosphonium bromide in 90% yield using Wittig chemistry according to a literature procedure.[48] 2-(*N*-Morpholino)ethyl methacrylate (MEMA) (Polysciences Inc.) was passed through a basic alumina column, then vacuum distilled over CaH_2 and stored at −20 °C prior to use. Copper(I) chloride, copper-(I) bromide, *N,N,N′,N′′,N′′*-pentamethyldiethylenetriamine (PM-DETA), 2,2′-bipyridine (bpy), 1,1,4,7,10,10-hexamethyltriethylene tetramine (HMTETA) and all other chemicals were purchased from Aldrich and used without further purification. The synthesis of poly-(4-vinylbenzoic acid)-*b*-poly(*N*-(morpholino)ethyl methacrylate) (VBA-*b*-MEMA) was described in detail previously.[21] VBA-*b*-MEMA block copolymer was obtained from the hydrolysis of the precursor block copolymer, poly(*tert*-butyl 4-vinylbenzoate)-*b*-poly(*N*-(morpholino)ethyl methacrylate) (*t*-BuVBA-*b*-MEMA). The mean degrees of polymerization (DP) of VBA and MEMA blocks are 66 and 123, respectively, as determined from the ^{1}H NMR analyses of the precursor block copolymer. THF GPC analysis of this diblock copolymer gave an M_n of 33 700 and an M_w/M_n of 1.08 compared against poly(methyl methacrylate) standards.

Laser Light Scattering (LLS). Dynamic LLS studies were performed on a Brookhaven Instruments Corp. BI-200SM goniometer equipped with a BI-9000AT digital correlator using a solid-state laser (125 mW, λ = 532 nm). The intensity-average hydrodynamic radius, $\langle R_h \rangle$, and polydispersity of the micelles were obtained by a cumulant analysis of the experimental correlation function.

Static LLS was performed using a DAWN DSP laser photometer, equipped with a 5 mW He–Ne laser (λ = 633 nm) and eighteen photodiode detectors at scattering angles ranging from 22.5° to 147°. In static light scattering, extrapolating the angular dependence of

CDV

Table 1. Structural Parameters of VBA−Core Micelles and "Inverted" MEMA−Core Micelles Formed by VBA$_{63}$-b-MEMA$_{123}$ Diblock Copolymers under Different Conditions

micelle parameters	VBA$_{63}$-b-MEMA$_{123}$ at pH 10, no Na$_2$SO$_4$[a]	VBA−core micelles at pH 2 and 0.8 M Na$_2$SO$_4$	MEMA−core micelles at pH 10 and 0.8 M Na$_2$SO$_4$
$M_{w,micelles}$	4.54×10^4	4.81×10^5	1.36×10^7
$\langle R_g \rangle$/nm			25
$\langle R_h \rangle$/nm	4	14[b]	33[b]
$\langle R_g \rangle / \langle R_h \rangle$			0.76
N_{agg}	1−2	11	299
$\langle \rho \rangle$/(g/cm^3)	/	0.07	0.15
scattering intensities (au)[c]	2.3	5.5	15.7

[a] Determined by LLS in the presence of 0.01 M NaCl. [b] The R_h values were obtained by extrapolation to zero angle. [c] Detected at a scattering angle of 90°.

the excess absolute time-averaged scattered light intensity, known as the Rayleigh ratio $R_{vv}(q)$, of a dilute polymer solutions to zero angle led to the apparent weight-average molar mass, $M_{w,app}$ and the root-mean square z-average radius of gyration, $\langle R_g^2 \rangle_z^{1/2}$ (or written as $\langle R_g \rangle$), where q is the scattering vector. The dn/dc values of diblock copolymer solutions comprising MEMA−core micelles at pH 10 and VBA−core micelles at pH 2 were measured at 20 °C using an Optilab DSP interferometric refractometer ($\lambda = 633$ nm).

Stopped-Flow Studies with Light-Scattering Detection.[43,47] Stopped-flow studies were carried out using a Bio-Logic SFM300/S stopped-flow instrument. The SFM-3/S contains three stepmotor-driven 10 mL syringes (S1, S2, S3) that can be operated independently to carry out single- or double-mixing. The SFM-300/S stopped-flow apparatus is attached to a MOS-250 spectrometer; kinetic data were fitted using a Biokine program supplied by Bio-Logic. For light scattering detection at a fixed scattering angle of 90°, both the excitation and emission wavelengths were adjusted to 335 nm with 10 nm slits. The dynamic trace at each composition is averaged from 15 to 20 successive shots. Using FC-08 or FC-15 flow cells, the typical dead times were 1.1 and 2.6 ms, respectively. The solution temperature was maintained at 25 °C by circulating water around the syringe chamber and the observation head. All solutions prior to loading into the motor-driven syringes were clarified by 0.45 μm Milliopore Nylon filters. After each day's experiments, the liquid paths of the stopped-flow were thoroughly flushed with water (4−5 times) and then ethanol. The absolute scattering intensities of pure water at a selected voltage (500 V) applied to the photomultiplier were recorded at the beginning of each day's work. Over a period of 1−2 weeks, this value may vary from 0.03 to 0.08 V, due to the contamination of the flow cell presumably caused by the absorption of trace amounts of polymer or dusts. If the recorded value is above this range (0.03−0.08 V), the flow cell need to be disassembled, flushed with concentrated HNO$_3$ and thoroughly cleaned. Although the amplitudes of kinetic traces will partially depend on the applied voltages, the cleanness of the liquid paths and flow cell, we find that the reliability of relaxation times obtained from kinetic traces is guaranteed, i.e., the relative changes of scattering light intensities with time is repeatable.

In principle, the stopped-flow experiment is quite simple.[49] The Bio-Logic SFM300 stopped-flow uses the drive motor to rapidly fire two solutions, contained in separate drive syringes driven by separate motors, into a mixing device. The solution mixture then flows into the observation cell, displacing the previous solution with freshly mixed solution. The volume of solution expended during each experiment is limited by the drive motors. In addition, a hard-stop was used. The fresh reactants in the observation cell are irradiated by a light source and detectors are mounted either perpendicular or parallel to the path of incoming light. The time dependence of various optical properties (absorbance, fluorescence, light scattering, turbidity, fluorescence anisotropy, etc.) can be measured. Regardless of the configuration of the stopped-flow cell, resolution is limited by the time required for the reactants to flow from the final point of mixing to the observation cell. This is known as the characteristic "dead time" of the instrument setup. The flow of liquid was controlled by the three separate motors and the hard-stop. Although the mixed solution is subject to large shear forces,

light scattering detection starts 1−3 ms (i.e., the dead time) after the hard-stop, thus it is assumed that these shear forces do not influence the aggregation (or dissociation) process(es).

Results and Discussion

The VBA-b-MEMA diblock copolymer exhibits intriguing "schizophrenic" micellization behavior upon dually playing with solution pH and salt (Na$_2$SO$_4$) concentrations.[21] In the absence of salt, the copolymer chain unimolecularly dissolve at pH 10−12 and form VBA−core micelles at pH 2. In the presence of 0.8 M Na$_2$SO$_4$, VBA−core and MEMA−core micelles are formed at pH 2 and pH 10, respectively (Figure 1). Table 1 summarizes the structural parameters of unimers, VBA−core micelles, and MEMA−core micelles at different conditions, as determined by dynamic and static LLS. Also shown in Table 1 are the scattered intensities of unimer and micellar solutions at a scattering angle of 90°. This can be used for reference in the subsequent stopped-flow experiments, which monitor the time dependence of scattered intensities at a scattering angle of 90°.

Starting from the unimer solution of the diblock copolymer at pH 10 and a concentration of 2 g/L, addition of Na$_2$SO$_4$ to a final concentration of 0.8 M or adjusting to pH 2 using HCl leads to almost instant (within a few seconds) appearance of bluish tinge in the solution, indicating the formation of MEMA−core and VBA−core micelles, respectively. It should be noted that the LLS measurements in Table 1 were conducted ∼3 h after the micelle formation at selected conditions (pH, Na$_2$SO$_4$ concentration); previously, we have assumed that after this period of storage, equilibrium micelles have been obtained.[21] Honda et al.[44,45] and Nose et al.[46] have studies the kinetics of temperature-induced formation of block copolymer micelles, and they found that it takes several days for the micelles to reach final equilibrium.

We then conducted dynamic LLS measurements immediately after changing the solution pH to 2 or adding Na$_2$SO$_4$ to a concentration of 0.8 M, which will induce the formation of VBA−core and MEMA−core micelles, respectively. To avoid large temperature variations, the sample preparation (by mixing prefiltered solutions), immediate transfer the optical tube (10 mm diameter) into the LLS apparatus, and subsequent LLS measurements were all done at room temperature (∼24 °C, air-conditioned). The first reliable point of LLS measurements was obtained ∼ 60 s after the micelle formation. LLS measurements were then conducted at extended times up to 4 h, it was found that for both the VBA−core and the MEMA−core micelles, scattered light intensities and micelle diameters fluctuate around a constant value and remain essentially unchanged. This indicates that for the VBA−core and the MEMA−core micelles, the formation kinetics is apparently complete within the first 1 min after changing the solvent quality.

In the pioneering work of Tuzar et al.,[43] they have studied the micellization kinetics of polystyrene-b-poly(hydrogenated
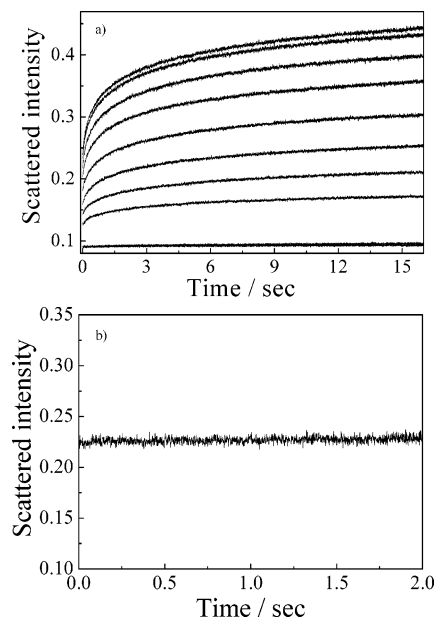
CDV

Figure 2. (a) Time dependence of the scattered light intensities of aqueous solutions of VBA-*b*-MEMA copolymer after a pH jump from 12 to 2 at 25 °C. From bottom to top, the final copolymer concentrations are 0.1, 0.2, 0.3, 0.4, 0.5, 0.6, 0.7, 0.8, 0.9, and 1.0 g/L, respectively. Initially, the diblock copolymer stock solution was at pH 12. (b) Time dependence of the scattered light intensity for a pH jump from 2 to 12 at 25 °C. The final copolymer concentration is 1.0 g/L.

isoprene) induced by a jump of the composition of mixed solvents (1,4-dioxane/heptane), and reported that the micellization is almost complete within 0.2−0.5 s. In our case, it is highly possible that during the final stages of micelle formation, the chains in the micelles will rearrange and take up more intertwined conformations in the micellar core. These conformational changes may continue for a rather long time scale, but would affect less the scattered light intensities and micelle diameters. We are currently employing pyrene end-labeled DHBCs to further probe this issue.

For the early stages of micelle formation, stopped-flow provides to be a suitable technique with a time resolution down to milliseconds,[43,47] which was used in subsequent kinetic studies. The time dependence of scattered light intensities at 90° was recorded following the abrupt jump of solution pH or/and salt concentrations via stopped-flow mixing.

Kinetics of the pH-Induced Formation and Breakup of VBA─Core Micelles. Figure 2a shows the time-dependent scattered light intensities obtained after stopped-flow mixing of aqueous VBA-*b*-MEMA copolymer solutions with HCl (initial pH 10, final pH 2; final copolymer concentrations = 0.1 to 1.0 g/L). At copolymer concentrations of up to 0.2 g/L, no relaxation was observed since rather flat dynamic plots were obtained. This critical concentration should be ascribed to the critical micellization concentration (cmc) for the VBA−core micelles of VBA-*b*-MEMA diblock copolymer at pH 2 and in the absence of salt. When the final copolymer concentrations were ≥0.3 g/L, light scattering intensities first increased abruptly with time and then gradually stabilized out after 8−10 s, suggesting the formation of VBA−core micelles.[21] It should be noted that at the longest measurement time of 16 s, scattering intensities still exhibit a small and gradual increase with time, especially at higher polymer concentrations (Figure 2a). This indicates that the final state of true equilibrium micelles has not been reached yet during this time period. The scattered light intensities stabilize at certain values after ~30−40 s, as revealed by stopped-flow measurements at extended times. However,
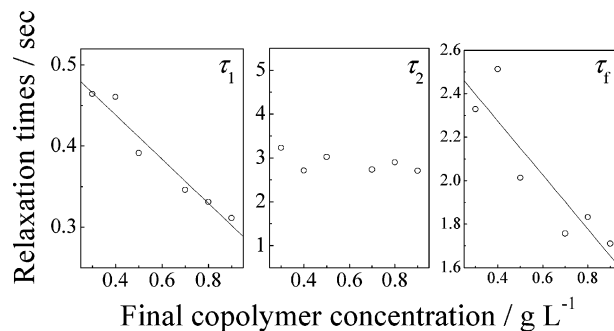

Figure 3. Double-exponential fitting results obtained from the micelle formation processes at different copolymer concentrations. The experimental conditions are the same as in Figure 2a.

most of the increase of scattered intensities (>90%) takes place within the first 16 s. The small increase of scattered light intensities at extended time period (16−30 s) is expected to be complicated by the dehydration and compaction of the micellar core, which will also lead to the moderate increase of scattered intensities. To extract more reliable kinetic information from the processes of unimer aggregation and micelle formation/breakup, only the kinetic data at early stages of micelle formation were analyzed, and the same principle was applied to all subsequent kinetic studies.

The time dependence of the scattered light intensity (I_t) can be normalized using $(I_\infty - I_t)/I_\infty$ vs t, where I_∞ is the value of I_t at infinitely long time. Such functions could only be well fitted by a double-exponential function

$$(I_\infty - I_t)/I_\infty = c_1 e^{-t/\tau_1} + c_2 e^{-t/\tau_2} \qquad (1)$$

where c_1 and c_2 are the normalized amplitudes and τ_1 and τ_2 are the characteristic relaxation times for two processes such that $\tau_1 < \tau_2$. The characteristic time for the overall process of micelle formation, τ_f, can be calculated as

$$\tau_f = c_1 \tau_1 + c_2 \tau_2 \qquad (2)$$

Figure 3 shows the fitting results for the dynamic traces (final copolymer concentration ≥ 0.3 g/L) shown in Figure 2a. Figure S1 in the Supporting Information shows the polymer concentration dependence of c_1 and c_2. Both τ_1 and τ_2 have positive amplitudes. τ_1 is in the range of 0.3−0.5 s and decreases with increasing copolymer concentration; τ_2 is ~3 s and is almost independent of the copolymer concentration in the range studied. The calculated τ_f for the overall micellization process ranges between 1.7 and 2.5 s, which decreases with increasing copolymer concentrations. The pH-induced kinetics of micelle formation of VBA-*b*-MEMA is quite comparable to that of GMA-*b*-DMA-*b*-DEA triblock copolymer as reported previously.[47] In the fast process (τ_1), unimers quickly associate into small aggregates and fusion between these small aggregates resulted in quasi-equilibrium micelles. The unimer concentration decreased rapidly close to the cmc after the fast process. The concentration-independent nature of τ_2 suggests that relaxation from quasi-equilibrium micelles to the final equilibrium micelles proceeded via unimer insertion/expulsion. Some quasi-equilibrium micelles dissociate, providing a reservoir of unimers. The overall effect is that the number density of micelles decreases and the average aggregation number per micelle increases until the system reaches its final equilibrium state, in which the rate of unimer entry equals that of unimer expulsion.

We then studied the kinetics of dissociation of VBA−core micelles into unimers when a micellar solution of VBA-*b*-
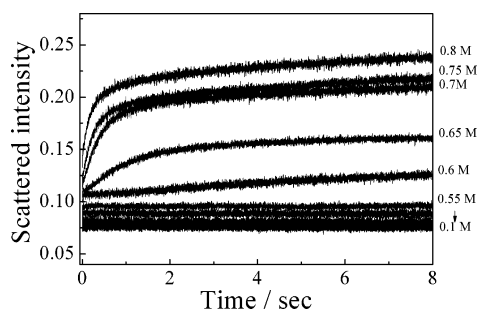
CDV

Figure 4. Time dependence of the scattered light intensities obtained after mixing an aqueous solution of VBA-*b*-MEMA copolymer with Na$_2$SO$_4$ using the stopped-flow technique at pH 10 and 25 °C. From bottom to top, the final Na$_2$SO$_4$ concentrations are 0.1, 0.2, 0.3, 0.4, 0.5, 0.55, 0.6, 0.65, 0.7, 0.75, and 0.8 M, respectively. The final copolymer concentration is fixed at 0.2 g/L.

MEMA copolymer at pH 2 was subjected to a pH jump from 2 to 12. A typical dynamic trace is shown in Figure 2b, scattering intensities remain as a flat line with time and no relaxation was observed, indicating that the dissociation of VBA−core micelles is complete within the dead time of the stopped-flow apparatus (∼2−3 ms). This is somewhat different from the kinetics of dissociation of GMA-*b*-DMA-*b*-DEA micelles induced by a pH jump from 2 to 12,[47] where a small decease in light scattering intensity was observed with a characteristic decay time of ∼100 ms, although most of signals were still lost within the dead time of stopped-flow apparatus.

Kinetics of the Salt-Induced Formation and Dilution-Induced Breakup of MEMA−Core Micelles. Figure 4 shows the time-dependent scattered light intensities obtained upon stopped-flow mixing an aqueous solution of VBA-*b*-MEMA copolymer with Na$_2$SO$_4$ at pH 10 and 25 °C. The final copolymer concentration was fixed at 0.2 g/L. If the final salt concentration is less than 0.6 M, the relaxation curve remains as a flat line, suggesting that the diblock copolymer chains are still molecularly dissolved, i.e., no micelles are formed. At a salt concentration of 0.6 M, the light scattering intensity increased moderately. At salt concentrations >0.65 M, scattering intensities abruptly increase and then reach a plateau within ∼1−2 s. This is due to the formation of MEMA−core micelles and the time scale (1−2 s) is consistent with the almost instantaneous appearance of bluish tinge after mixing. The critical salt concentration needed for the formation of MEMA−core micelles is in excellent agreement with that obtained from our previous dynamic LLS studies.[21]

Figure 4 also indicates that the MEMA−core micelles are formed much quicker at higher salt concentration. The dynamic trace obtained in the presence of 0.65 M Na$_2$SO$_4$ can be fitted with a single-exponential function. In the presence of >0.65 M Na$_2$SO$_4$, dynamic traces can only be well-fitted with double-exponential functions. Figure 5 shows the fitting results: τ_1, τ_2, and τ_f all decrease with increasing Na$_2$SO$_4$ concentration. The driving force for the formation of MEMA−core micelles is the addition of Na$_2$SO$_4$, thus it is quite understandable that the larger the driving force, the faster the micellization kinetics.

Figure 6 shows the time dependence of the scattered light intensity upon stopped-flow mixing aqueous solutions of VBA-*b*-MEMA copolymer at different concentrations with Na$_2$SO$_4$, and the final Na$_2$SO$_4$ concentration was fixed at 0.8 M. If the final copolymer concentration is ≤0.1 g/L, the dynamic curve remains linear, suggesting that no MEMA−core micelles are formed under these conditions (pH 10, 0.8 M Na$_2$SO$_4$). When the copolymer concentration is ≥0.15 g/L, an increase in light scattering intensity can be clearly observed.
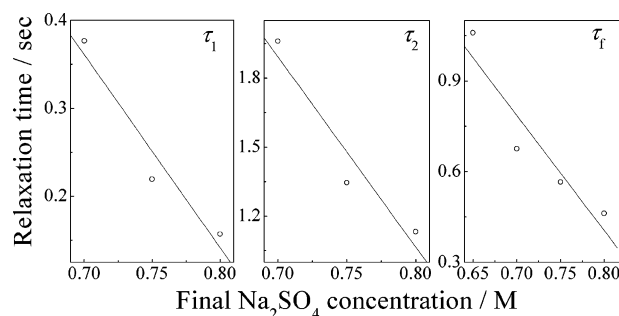

Figure 5. Double-exponential fitting results obtained for the formation of MEMA−core micelles at various Na$_2$SO$_4$ concentrations. The experimental conditions are the same as in Figure 4. The dynamic curve obtained in the presence of 0.65 M Na$_2$SO$_4$ is fitted with a single-exponential function.
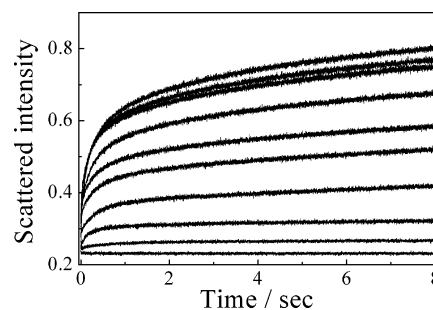

Figure 6. Time dependence of the scattered light intensities obtained after mixing an aqueous solution of VBA-*b*-MEMA copolymer with Na$_2$SO$_4$ using the stopped-flow technique at pH 10 and 25 °C. From bottom to top, the final diblock copolymer concentrations are 0.1, 0.15, 0.2, 0.4, 0.5, 0.6, 0.7, 0.8, 0.9, and 1.0 g/L, respectively. The final Na$_2$SO$_4$ concentration is fixed at 0.8 M.
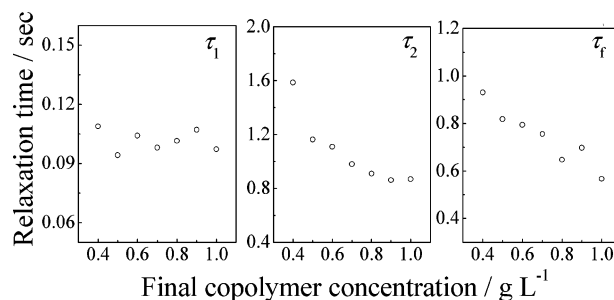

Figure 7. Double-exponential fitting results obtained for the formation of MEMA−core micelles at different copolymer concentrations. The experimental conditions are the same as in Figure 6.

Figure 7 shows the double-exponential fitting results of the dynamic traces reported in Figure 6. The polymer concentration dependence of c_1 and c_2 are shown in Figure S2 in the Supporting Information. τ_1 is ∼0.1 s and barely changes with copolymer concentrations. τ_2 is in the range of 0.8−1.6 s and decreases with increasing copolymer concentration. The calculated τ_f for the overall salt-induced micellization process is ∼0.5−1.0 s. The salt-induced formation of MEMA−core micelles also proceeds via two successive steps. Dormidontova et al.[40−42] predicted that, in the first (fast) stage of micellization, unimers quickly associate to form small nascent micelles, then slow fusion between these nascent micelles results in the formation of quasi-equilibrium micelles. During the initial fast process, unimer insertion/expulsion contributes little toward micellization, because the activation energy is relatively high for unimer release from small micelles. They also predicted that, in the second slow process, the unimer insertion/expulsion mechanism would dominate. However, in our case, the decrease of τ_2 with increasing copolymer concentration suggests that
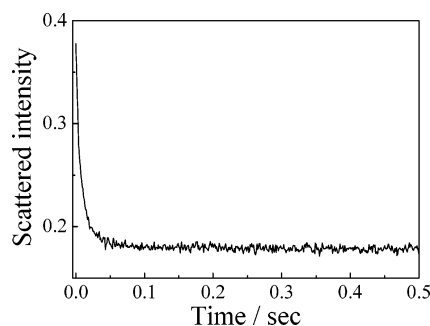
CDV

Figure 8. Time dependence of the scattered light intensity obtained after diluting an aqueous solution of VBA-*b*-MEMA copolymer (initially at 1.0 g/L with 0.8 M Na$_2$SO$_4$) with an equal volume of water at pH 10.
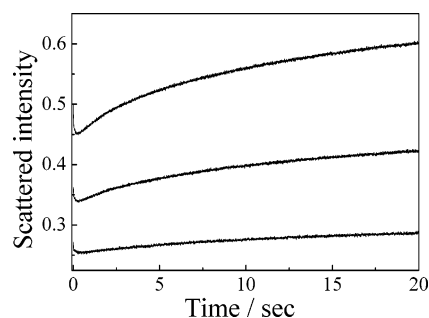

Figure 9. Typical time dependence of the scattered light intensities obtained for three aqueous VBA-*b*-MEMA copolymer solutions after a pH jump from 2 to 12 at 25 °C in the presence of 0.8 M Na$_2$SO$_4$. From bottom to top, the final copolymer concentrations are 0.2, 0.3, and 0.5 g/L, respectively. Initially, the diblock copolymer stock solution was at pH 2.

micelle fusion/fission mechanism also dominate during the second slow process; this is probably due to the high concentration of salt. For the micellization dynamics of small molecule surfactant in the presence of salt, micelle fusion/fission also dominates during the slow process of micelle formation/breakup.[27,28]

A comparison between the results shown in Figure 3 and Figure 7 revealed that the formation of MEMA−core micelles is much quicker than that of the VBA−core micelles. This could be at least partially due to the chain length asymmetry of the VBA and MEMA blocks (Table 1). The dissociation of MEMA−core micelles into unimers can be conveniently induced by dilution with water, because no micelles exist at 25 °C when the Na$_2$SO$_4$ concentration is less than 0.6 M.[21] Figure 8 shows a typical dynamic trace obtained when MEMA−core micelles (1.0 g/L copolymer in 0.8 M Na$_2$SO$_4$) were diluted with an equal volume of water. The entire breakup kinetics MEMA−core micelles was observed, which is in striking contrast to the pH-induced breakup of DEA−core micelles of GMA-*b*-DMA-*b*-DEA triblock copolymer[47] or VBA−core micelles of VBA-*b*-MEMA. The dynamic traces shown in Figure 8 can be readily fitted with a single-exponential function. This analysis yielded a characteristic relaxation time (τ_d) of ∼8 ms and the micelle dissociation was complete within 50 ms.

During the pH-induced micelle breakup, the core block is instantaneously ionized, and the charge repulsion between chain segments from the same or different polymer chains perhaps contribute to the fast dissociation into unimers. In the dilution-induced breakup of MEMA−core micelles, the MEMA block in the core keeps neutral. We thus can imagine that its dissociation into unimers should be slower. The MEMA−core micelles have an intensity-average diameter of ∼66 nm, with a micelle aggregation number (N_{agg}) of ∼300; while the diameter of VBA−core micelles is ∼28 nm, with a N_{agg} of ∼11 (Table 1). The MEMA−core micelles have a chain density of 0.15 g/cm^3, which is almost twice as that of the VBA−core micelles (0.07 g/cm^3).[21] The relatively slow breakup of MEMA−core micelles into unimers may also suggests interchain entanglements of the MEMA blocks inside the micelle core. This is feasible given that the mean degree of polymerization of the MEMA block is 123. Chain entanglements inside the VBA cores are less likely given the much lower aggregation number of these micelles and the significantly lower mean degree of polymerization of the VBA block.

Kinetics of Structural Inversion from VBA━Core to MEMA━Core Micelles. In the presence of 0.8 M salt, VBA−core micelles are formed at pH 2 and MEMA−core micelles are formed at pH 12, thus a convenient pH jump will lead to the structural inversion between VBA−core and MEMA−core

micelles. One important question is as follows. Will the kinetics of structural inversion between VBA−core and MEMA−core micelles be different from that of the unimer−micelle transition? In principle, the pH-induced structural inversion between the two micelle states (i.e., VBA−core and MEMA−core micelles) can proceed via three possible mechanisms. The first involves micelle dissociation to give unimers (if the core becomes hydrophilic before the coronal chains become hydrophobic), followed by remicellization. The second involves micelle flocculation (if the coronal chains become hydrophobic before the core chains become hydrophilic), followed by (or perhaps at the same time as) micelle inversion. The third possibility is simply micelle inversion (i.e., the core chains become hydrophilic on the same time scale that the coronal chains become hydrophobic, without any loss of micelle stability).

Figure 9 shows the typical time-dependent scattered light intensities recorded during structural inversion from VBA−core to MEMA−core micelles induced by a pH jump from 2 to 12 in the presence of 0.8 M Na$_2$SO$_4$. Interestingly, an initial rapid decrease in scattered light intensity occurrs within the first ∼0.2 s; on longer time scales, the scattering intensities gradually increase and then stabilize out. The initial decrease of scattered intensities should be due to the dissociation of VBA−core micelles into unimers. In the absence of salt, the breakup of VBA−core micelles into unimers upon a pH jump from 2 to 12 occurs within 2−3 ms. It seems that the presence of 0.8 M Na$_2$SO$_4$ significantly retards the kinetics of micelle dissociation.

The scattered intensity after the initial rapid decrease remains relatively high compared to that of the aqueous solution of individual VBA-*b*-MEMA chains at pH 12 in the absence of salt. Moreover, the intensity at the starting point ($t = 0$, which is actually 2.6 ms after pH jump) is also much larger than that of the VBA−core micelles at the same concentration and pH 2 (Figure 2a). The above observations indicate that the micelle inversion from VBA−core to MEMA−core micelles is quite complex.

Immediately upon jumping the solution pH from 2 to 12, instantaneous deprotonation of the MEMA block renders the MEMA shell of VBA−core micelles insoluble. Translational diffusion of micellar particles will lead to intermicelle collisions, which will effectively lead to micellar fusion due to the insolubility of the coronal MEMA chains. The characteristic time for diffusion-limited aggregation between VBA−core micelles is given by $\tau_{agg} \approx {}^1\!/_4\pi DRc \approx 3\eta/2ck_BT$,[50] where c is the number of micelles per unit volume. The value of c can be estimated from the total copolymer concentration and mean micelle aggregation number (Table 1). The translational diffusion coefficient, D, is given by the Stokes−Einstein equation
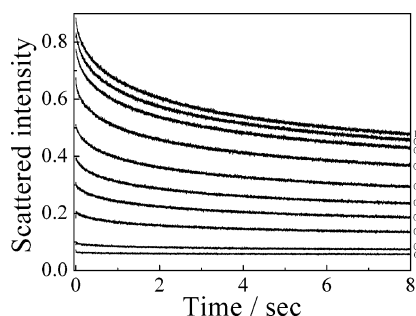
CDV

Figure 10. Time dependence of the scattered light intensities obtained after a pH jump from 12 to 2 at 25 °C in the presence of 0.8 M Na$_2$SO$_4$. From bottom to top, the final copolymer concentrations are 0.1, 0.2, 0.3, 0.4, 0.5, 0.6, 0.7, 0.8, 0.9, and 1.0 g/L, respectively. Initially, the diblock copolymer stock solution was at pH 12.
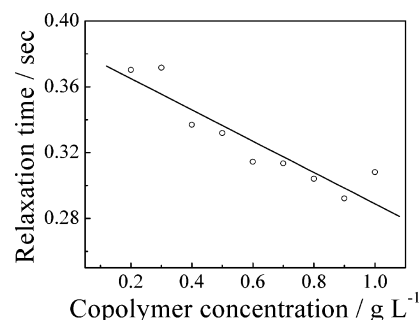

Figure 11. Single-exponential fitting results obtained for the micelle inversion from MEMA−core micelles to VBA−core micelles at various copolymer concentrations. The experimental conditions are the same as those shown in Figure 10.

$D = k_B T/6\pi\eta R_h$, where k_B is the Boltzmann constant, and η is the solvent viscosity (which is 8.9 × 10^{-3} P for water at 25 °C). At a final copolymer concentration of 0.5 g/L, τ_{agg} is ∼0.05 ms. This indicates that within the dead time of the stopped-flow (2−3 ms), intermicelle collision of VBA−core micelles will surely take place, a considerable fraction of this type of collision will lead to partial fusion between VBA−core micelles due to the insolubility of MEMA shell at pH 12 in the presence of 0.8 M Na$_2$SO$_4$. This well explains the relatively large scattered light intensities at $t = 0$ (2.6 ms after the pH-jump).

We can imagine that the initial fusion between VBA−core micelles within the dead time of stopped-flow will lead to the formation of loose aggregates. During the same time scale, the VBA block in the micelle core will be ionized and become well-solvated, leading to the dissociation of isolated VBA−core micelles into unimers and the partial disintegration of the loose aggregates resulting from the fusion of VBA−core micelles. However, this process is complicated by the reassembly of dissociated unimers into MEMA−core micelles.

It is a good estimate that during the first 0.2 s after pH jump, the breakup of the VBA−core micelles into unimers and the partial disintegration of loose aggregates from micelle fusion dominates over the reaggregation of unimer chains into MEMA−core micelles. After this time period, the solvation of the VBA−core is almost complete. The structural rearrangement of loose aggregate due to fusion of VBA−core micelles and the reaggregation of unimer chains into MEMA−core micelles then become dominant in subsequent processes, leading to the gradual increase of scattered intensities. This explanation is thus consistent with the relatively large scattered intensities immediately after pH jump (at $t = 0$), the rapid decrease within the first 0.2 s, and the subsequent gradual increase of the scattered light intensities.

Figure 9 also shows the dynamic traces of the micellar inversion from VBA−core to MEMA−core micelles at different polymer concentrations. It was found for all the 3 different concentrations, the initial rapid decrease of scattered intensities takes place within almost the same time period of ∼ 0.2 s. This again confirms that the decrease is due to the VBA core-solvating after pH jump, which should be independent of polymer concentrations.

Kinetics of Structural Inversion from MEMA━Core to VBA━Core Micelles. Figure 10 shows the typical time dependence of the scattered light intensity after stopped-flow mixing an aqueous VBA-*b*-MEMA copolymer solution with HCl at 25 °C in the presence of 0.8 M Na$_2$SO$_4$. All the dynamic traces exhibit negative amplitudes. The kinetics of dissociation of MEMA−core micelles into individual chains induced by

dilution at pH 10 have already been examined (Figure 8), and this breakup process is almost complete within ∼50 ms.

All the dynamic traces shown in Figure 10 can be well fitted with single-exponential functions, suggesting a different mechanism to that observed for unimer-to-micelle transitions (see Figures 2a and 6). The characteristic relaxation time for micelle structural inversion (τ_i) is ∼0.3 s; this decay time decreases slightly with copolymer concentration (Figure 11).

Upon jumping from pH 12 to 2, MEMA−core micelles undergo structural inversion into VBA−core micelles. The MEMA−core micelles are larger, denser, and scatter much more light compared to VBA−core micelles (Table 1). The characteristic time for diffusion-limited aggregation, τ_{agg}, between MEMA−core micelles is calculated to be ∼1.5 ms,[50] so the micelle fusion between MEMA−core micelles due to the insolubility of VBA shell at pH 2 is not prominent. We do not observe an initial rapid decrease of scattering intensities as in the case of structural inversion from VBA−core to MEMA−core micelles (Figure 9). This presumably suggests that the rapid dissociation of MEMA−core micelles into unimer chains may not take place. We then tentatively propose that the structural inversion will proceeds first with the splitting of large MEMA−core micelles into small VBA−core micelles, followed and/or accompanied by the redistribution of unimer chains between appearing small VBA−core micelles.

Conclusions

In summary, the micellization kinetics of a "schizophrenic" zwitterionic diblock copolymer, poly(4-vinylbenzoic acid)-*b*-poly(*N*-(morpholino)ethyl methacrylate) (VBA-*b*-MEMA), have been studied in detail. In particular, the kinetics of pH-induced formation and dissociation of VBA−core micelles, the salt-induced formation and dilution-induced dissociation of MEMA−core micelles at pH 10, and pH-induced micellar inversion between VBA−core and MEMA−core micelles in the presence of 0.8 M Na$_2$SO$_4$ were examined by a stopped-flow light scattering technique. A pH jump from 12 to 2 in the absence of salt leads to the formation of VBA−core micelles from individual copolymer chains. For the complementary pH jump from 2 to 12, the dissociation of VBA−core micelles into unimers occurs within the dead time for the stopped-flow cell (∼2−3 ms). At pH 10, addition of Na$_2$SO$_4$ (>0.6 M) caused the formation of MEMA−core micelles. The dynamic traces obtained at ≥0.7 M Na$_2$SO$_4$ can be well fitted with double-exponential functions, leading to both fast (τ_1) and slow (τ_2) relaxation times. τ_1 is in the range 0.1−0.4 s and τ_2 is in the range 1−2 s. Both τ_1 and τ_2 decrease with increasing Na$_2$SO$_4$ concentration, providing a stronger driving force for salt-induced micellization. The copolymer concentration dependences of τ_1

CDV

and τ_2 for a salt jump from 0 to 0.8 M Na_2SO_4 reveals that the fast process (τ_1) corresponds to the rapid aggregation of unimers into quasi-equilibrium micelles with a mean micelle aggregation number (N_{agg}) that is lower than that of the equilibrium micelles; the slow process (τ_2) is ascribed to micelle formation and breakup, which proceeds mainly through micelle fusion/fission. The dilution-induced transition from MEMA−core micelles to unimers typically occurs within 50 ms, with a characteristic relaxation time of ∼8 ms.

Structural inversion between the MEMA−core and VBA−core micelles in the presence of 0.8 M Na_2SO_4 was achieved by a pH jump from 12 to 2 and vice versa. For the structural inversion from VBA−core to MEMA−core micelles, the insolubility of MEMA shell at pH 12 leads to partial fusion of VBA−core micelles within the stopped-flow dead time (2−3 ms), leading to relatively high scattering intensities at $t = 0$ as compared to the original VBA−core micelles at pH 2. The scattering intensities then typically exhibit a rapid decrease within the first ∼0.2 s and then gradually increase again. The initial decrease in the scattered light intensity suggests rapid dissociation of the VBA−core micelles into unimers and partial disintegration of loose aggregates resulting from fusion between VBA−core micelles. The structural rearrangement of loose aggregate and the reaggregation of unimer chains into MEMA−core micelles then become dominant in subsequent processes, leading to the gradual increase of scattered intensities. In contrast, the structural inversion from MEMA−core to VBA−core micelles exhibits different pathways. The scattered light intensities decrease monotonically with time before stabilizing out, indicating that the rapid dissociation into individual chains does not occur. The relaxation curves can be well-fitted using a single-exponential function. The decay constant τ is ∼0.3 s, which slightly decreases with increasing copolymer concentration. A micelle splitting mechanism for the structural inversion from MEMA−core to VBA−core micelles is tentatively proposed.

Supporting Information Available: Figures showing double exponential fitting results (c_1 and c_2) of kinetic traces of the formation of VBA−core and MEMA−core micelles at different copolymer concentrations. This material is available free of charge via the Internet at http://pubs.acs.org.

References and Notes

(1) Hamley, I. W. *The Physics of Block Copolymers*; Oxford University Press: Oxford, U.K., 1998.
(2) Fustin, C. A.; Abetz, V.; Gohy, J. F. *Eur. Phys. J. E* **2005**, *16*, 291−302.
(3) Gohy, J. F. *Adv. Polym. Sci.* **2005**, *190*, 65−136.
(4) Hadjichristidis, N.; Iatrou, H.; Pitsikalis, M.; Pispas, S.; Avgeropoulos, A. *Prog. Polym. Sci.* **2005**, *30*, 725−782.
(5) Riess, G. *Prog. Polym. Sci.* **2003**, *28*, 1107−1170.
(6) Rodriguez-Hernandez, J.; Checot, F.; Gnanou, Y.; Lecommandoux, S. *Prog. Polym. Sci.* **2005**, *30*, 691−724.
(7) Colfen, H. *Macromol. Rapid Commun.* **2001**, *22*, 219−252.
(8) Butun, V.; Billingham, N. C.; Armes, S. P. *J. Am. Chem. Soc.* **1998**, *120*, 11818−11819.
(9) Rodriguez-Hernandez, J.; Lecommandoux, S. *J. Am. Chem. Soc.* **2005**, *127*, 2026−2027.
(10) Maeda, Y.; Mochiduki, H.; Ikeda, I. *Macromol. Rapid Commun.* **2004**, *25*, 1330−1334.
(11) Arotcarena, M.; Heise, B.; Ishaya, S.; Laschewsky, A. *J. Am. Chem. Soc.* **2002**, *124*, 3787−3793.
(12) Virtanen, J.; Arotcarena, M.; Heise, B.; Ishaya, S.; Laschewsky, A.; Tenhu, H. *Langmuir* **2002**, *18*, 5360−5365.
(13) Andre, X.; Zhang, M. F.; Muller, A. H. E. *Macromol. Rapid Commun.* **2005**, *26*, 558−563.
(14) Schilli, C. M.; Zhang, M. F.; Rizzardo, E.; Thang, S. H.; Chong, Y. K.; Edwards, K.; Karlsson, G.; Muller, A. H. E. *Macromolecules* **2004**, *37*, 7861−7866.
(15) Gil, E. S.; Hudson, S. A. *Prog. Polym. Sci.* **2004**, *29*, 1173−1222.
(16) Alarcon, C. D. H.; Pennadam, S.; Alexander, C. *Chem. Soc. Rev.* **2005**, *34*, 276−285.
(17) Dai, S.; Ravi, P.; Tam, K. C.; Mao, B. W.; Gang, L. H. *Langmuir* **2003**, *19*, 5175−5177.
(18) Gan, L. H.; Ravi, P.; Mao, B. W.; Tam, K. C. *J. Polym. Sci., Part A: Polym. Chem.* **2003**, *41*, 2688−2695.
(19) Butun, V.; Liu, S.; Weaver, J. V. M.; Bories-Azeau, X.; Cai, Y.; Armes, S. P. *React. Funct. Polym.* **2006**, *66*, 157−165.
(20) Liu, S. Y.; Armes, S. P. *Angew. Chem., Int. Ed.* **2002**, *41*, 1413−1416.
(21) Liu, S. Y.; Armes, S. P. *Langmuir* **2003**, *19*, 4432−4438.
(22) Liu, S. Y.; Billingham, N. C.; Armes, S. P. *Angew. Chem., Int. Ed.* **2001**, *40*, 2328−2331.
(23) Weaver, J. V. M.; Armes, S. P.; Butun, V. *Chem. Commun.* **2002**, 2122−2123.
(24) Aniansson, E. A. G.; Wall, S. N. *J. Phys. Chem.* **1974**, *78*, 1024−1032.
(25) Aniansson, E. A. G.; Wall, S. N. *J. Phys. Chem.* **1975**, *79*, 857−858.
(26) Aniansson, E. A. G.; Wall, S. N.; Almgren, M.; Hoffmann, H.; Kielmann, I.; Ulbricht, W.; Zana, R.; Lang, J.; Tondre, C. *J. Phys. Chem.* **1976**, *80*, 905−922.
(27) Kahlweit, M. *J. Colloid Interface Sci.* **1982**, *90*, 92−99.
(28) Lessner, E.; Teubner, M.; Kahlweit, M. *J. Phys. Chem.* **1981**, *85*, 1529−1536.
(29) Patist, A.; Kanicky, J. R.; Shukla, P. K.; Shah, D. O. *J. Colloid Interface Sci.* **2002**, *245*, 1−15.
(30) Lang, J.; Zana, R. *Surfactant Solutions: New Methods of Investigation.* Marcel Dekker: New York, 1987.
(31) Halperin, A.; Alexander, S. *Macromolecules* **1989**, *22*, 2403−2412.
(32) Goldmints, I.; Holzwarth, J. F.; Smith, K. A.; Hatton, T. A. *Langmuir* **1997**, *13*, 6130−6134.
(33) Michels, B.; Waton, G.; Zana, R. *Langmuir* **1997**, *13*, 3111−3118.
(34) Goldmints, I.; von Gottberg, F. K.; Smith, K. A.; Hatton, T. A. *Langmuir* **1997**, *13*, 3659−3664.
(35) Kositza, M. J.; Bohne, C.; Alexandridis, P.; Hatton, T. A.; Holzwarth, J. F. *Macromolecules* **1999**, *32*, 5539−5551.
(36) Kositza, M. J.; Bohne, C.; Alexandridis, P.; Hatton, T. A.; Holzwarth, J. F. *Langmuir* **1999**, *15*, 322−325.
(37) Waton, G.; Michels, B.; Zana, R. *Macromolecules* **2001**, *34*, 907−910.
(38) Kositza, M. J.; Bohne, C.; Hatton, T. A.; Holzwarth, J. F. *Trends Colloid Interface Sci.* **1999**, *112*, 146−151.
(39) Wang, Y. M.; Mattice, W. L.; Napper, D. H. *Langmuir* **1993**, *9*, 66−70.
(40) Dormidontova, E. E. *Macromolecules* **1999**, *32*, 7630−7644.
(41) Esselink, F. J.; Dormidontova, E.; Hadziioannou, G. *Macromolecules* **1998**, *31*, 2925−2932.
(42) Esselink, F. J.; Dormidontova, E. E.; Hadziioannou, G. *Macromolecules* **1998**, *31*, 4873−4878.
(43) Bednar, B.; Edwards, K.; Almgren, M.; Tormod, S.; Tuzar, Z. *Makromol. Chem.−Rapid Commun.* **1988**, *9*, 785−790.
(44) Honda, C.; Abe, Y.; Nose, T. *Macromolecules* **1996**, *29*, 6778−6785.
(45) Honda, C.; Hasegawa, Y.; Hirunuma, R.; Nose, T. *Macromolecules* **1994**, *27*, 7660−7668.
(46) Iyama, K.; Nose, T. *Macromolecules* **1998**, *31*, 7356−7364.
(47) Zhu, Z. Y.; Armes, S. P.; Liu, S. Y. *Macromolecules* **2005**, *38*, 9803−9812.
(48) Ishizone, T.; Hirao, A.; Nakahama, S. *Macromolecules* **1989**, *22*, 2895−2901.
(49) Johnson, K. A. *Kinetic Analysis of Macromolecules: A Practical Approach.* Oxford University Press: New York, 2003.
(50) Chu, B.; Ying, Q. C.; Grosberg, A. Y. *Macromolecules* **1995**, *28*, 8, 180−189.